A hybrid system-level prognostics approach with online RUL forecasting for electronics-rich systems with unknown degradation behaviors

Ahmad Al-Mohamad[a,b,*], Ghaleb Hoblos[a], Vicenç Puig[b]

[a] Normandy University, UNIROUEN, ESIGELEC, IRSEEM, 76000 Rouen, France
[b] Universitat Politècnica de Catalunya (UPC), Campus de Terrassa, Rambla Sant Nebridi, 10, 08222, Spain

ARTICLE INFO

Keywords:
Model-based prognostics
Parameter estimation
Power electronics
Prediction algorithms
Prognostics and health management
Reliability assessment
Remaining useful life

ABSTRACT

This paper proposes a system-level prognostic approach for power electronic systems with slow degradation profiles. Although a model-based approach has been adopted to deal with such multivariable dynamical systems with degradation properties, the forecasting of the Remaining Useful Life (RUL) is independent of prior knowledge of degradation profiles. Thus, this proposition is mainly based on the estimation of the degraded parameters. A robust and well-known technique, the Adaptive Joint Extended Kalman Filter (AJEKF), has been used in previous publications for degradation estimation. Consequently, a deep comprehension of the fault mechanisms of the critical electronic components such as Electrolytic Capacitors (ECaps) and power switching devices such as MOSFETs is needed to define their fault precursors and their degradation behaviors for analytical modeling. The developed forecasting methodology highlights the importance of the historical degradation data in the modeling and estimation stages. The main goal is to increase the reliability of the Prognostics and Health Management (PHM). Thus, this technique has been fully applied to a DC-DC converter used in electric vehicles to forecast its RUL on system-level from component-level basis and the simulation results are then presented.

1. Introduction

Electronics-rich systems are interestingly gaining attention in some applications with critical decisions and harsh operating conditions. Their increasing important role in critical applications such as electric vehicles, aircrafts industry and huge industrial applications lead the scientific researchers to consider the reliability assessment study which helps to provide high operational availability [1,2]. Mainly, faults and scheduled maintenance could affect the operation of such systems. In this study, only faults with slow degradation profiles are considered to be predicted. Thus, the intermittent faults could not be considered in such studies due to their unpredictable occurrence [3]. Harsh environmental and working conditions could be described as thermal and electrical overstresses which will affect the reliability of the system during the time and lead to a complete failure [4,5]. Consequently, targeting high efficiency and reliability in electronics-rich systems needs high-fidelity modeling, advanced monitoring, diagnosis and preventive maintenance techniques and strategies which all could be followed in an organized and specific Prognostics and Health Management (PHM) methodology. The methodologies and techniques on which the diagnostics rely are considered as strong enough to be standardized. However, there is not a single methodology that discusses and covers all the prognostics aspects so far. Thus, the prognostics technology is changing the health management standards and considered as the most challenging in the domain [6].

The failures in power electronics systems and their consequences have been widely discussed in [7–9]. To be more specific, in the literature there exists component-level approaches for prognostics as in [4,5,10] for ECaps and in [11–13]. Their proposed methods normally require the failure modes derived from statistical studies, designers, reliability engineers, measurements and Accelerated aGing Tests (AGE). Therefore, the common behavior in the followed prognostics techniques is that a damage estimation is vital at a certain level for the RUL prediction. Thus, they propose filter approaches for damage estimation such as Kalman and particle filters depending on the complexity of the system and its type. Additionally, for the RUL prediction they use the degradation models in order to predict their future states subject to current degradation estimation and other measurements. Based on these algorithms, the degradation models and trends should be known for each and every parameters in the system, which also could give

* Corresponding author at: Normandy University, UNIROUEN, ESIGELEC, IRSEEM, 76000 Rouen, France. Universitat Politècnica de Catalunya (UPC), Campus de Terrassa, Rambla Sant Nebridi, 10, 08222, Spain.

E-mail addresses: ahmad.al-mohamad@univ-rouen.fr (A. Al-Mohamad), ghaleb.hoblos@esigelec.fr (G. Hoblos), vicenc.puig@upc.edu (V. Puig).

URL: https://www.researchgate.net/profile/Ahmad_Al_Mohamad (A. Al-Mohamad).

efficient estimation and prediction results but limited by the knowledge of the degradation models. There exist also other RUL prediction methods that do not require prior knowledge of the degradation profiles and applied on mechanical systems as in [14,15] which are based on the degradation speed and its distance from the ideal parameter value. Although these prediction techniques have shown efficient results, one depends on full knowledge of the degradation profile and works on a component-level prognostics and the second requires real-time measurements for monitoring process in addition to the ideal case for the RUL computation.

In this context, this paper contributes to the PHM with a different point of view. First, it aims to deal with a multicomponent approach instead of single-component which also can be called system-level prognosis, for more robustness, better reliability and projection to realistic applications. Second, the RUL prediction is only based on the degradation estimation with unknown degradation behaviors. Explicitly, the stochastic estimators as Kalman Filter (KF) deal with linear systems in presence of Gaussian white noises, whereas for nonlinear systems, Extended Kalman Filter (EKF) can be applied by computing the covariances using Jacobian of nonlinear functions. Moreover, the prediction matrices are updated by real-time measurements with stochastic noises. Therefore, a power electronic system is adopted as a case study for the proposed PHM methodology. Thus, the system is modeled and described as Linear Parameter Variant (LPV) dynamical system due to the degradation of the parameters over time. Furthermore, a proposition of a three-stage PHM methodology has taken place in this study in order to achieve the aforementioned RUL prediction goals. In addition to the model-based approach, statistical degradation data are needed to create analytical models for each and every degraded parameter in order to infect the healthy system with slow degradation profiles. The latter is only needed in the absence of real application, and the goal here is to validate the proposed methodology by running and testing the studied system in simulation. There exists an open access database for the failure mechanisms and measurements of the most critical power electronic devices provided by Nasa prognostics center.

This paper points out the necessity of system-level PHM and proposes a methodology for model-based prognostics and RUL forecasting for systems with unknown degradation behaviors. Thus, Section 2 states the concerned problem and explains the scientific contribution of the work. The application to a DC-DC converter with both healthy and degraded operations is presented in Section 3. In the absence of the real system, it is important to understand the failure mechanisms of the power electronic devices and model their degradation for simulation validations which Section 4 explicitly explains. Section 5 is dedicated for the proposed PHM algorithm and the RUL prediction. The simulation results are analyzed and explained in Section 6. Finally, the conclusions and perspectives are provided in the last section.

2. Problem statement

Since the safety in critical engineering process and applications plays an important role in the maintenance of the systems, the system operation should be continuously monitored to avoid catastrophic lives losses and project abortions. Thus, ensuring the reliable operations counts on the system failure mechanisms probabilities and online surveying. Consequently, the prognostics techniques intend to forecast the RUL either by model-based or data-driven methods, depending on the probability of faults and the complexity of systems. Moreover, the PHM takes place to resolve the problems of cut-offs due to optimistic protection and expensive maintenance caused by over-protection.

Environmental aspects such as temperature and working conditions affect the system functionality and availability. Considering the electronics-rich systems such as DC-DC converters, the working conditions are described as voltage surges, current overshoots and high temperature causing system failures. Mainly, two principal components are responsible of the failure of the such converters, the switching devices and ECaps [16]. Hence, a problem of inter-dependency of those components arises and predicting the health of the system becomes more complex. Additionally, most of the systems might be treated as black boxes with unknown parameters, which turns the problem into higher level prognosis for RUL prediction with unknown degradation profiles. Section 5 explicitly explains the proposed algorithm of the complete PHM technique from modeling to online RUL prediction. Moreover, a vital estimation-based technique is integrated to overcome the lack of measurements information in any electronics-rich system.

Fig. 1 illustrates the problem statement and resumes the PHM architecture to reach the main objective of online RUL estimation for system-level prognosis.

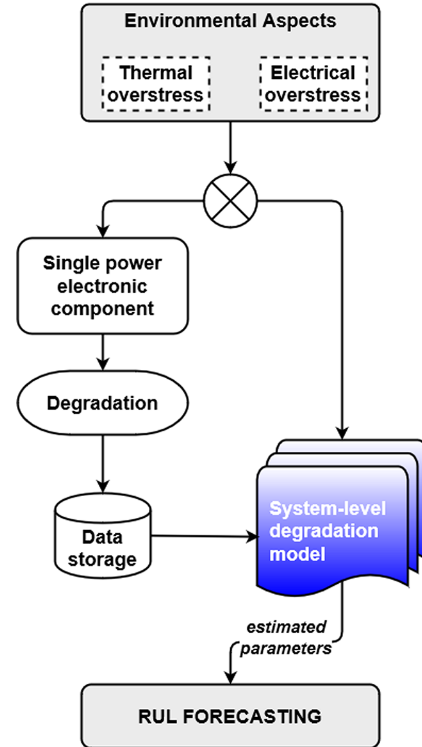

Fig. 1. Problem statement of the system-level PHM.

3. DC-DC converter case study

Switch-mode power converters are widely used in EVs as bi-directional buck-boost converters. Thus, they experience environmental as well as operational stress such as heat, current spikes and voltage surges [4]. Hence, these factors affect the proper operating conditions of the converters and deteriorate the efficiency of the system including the internal components. Therefore, the reliability of the system would not be trustworthy in huge industrial applications such as nuclear power plants and autonomous vehicles. Consequently, the PHM would prevent these systems from unnecessary and expensive maintenance [17].

3.1. Boost converter modeling

A bi-directional buck-boost converter would reflect a perfect application of the PHM algorithms. A DC-DC converter, rated at 30 kW, is designed as shown in Fig. 2. For the sake of simplification, only the Boost application is explained in this paper.

The components parameters and variables are presented in Table 1.

Consider the state-space model of a continuous-time switched linear system in normal operation as follows:

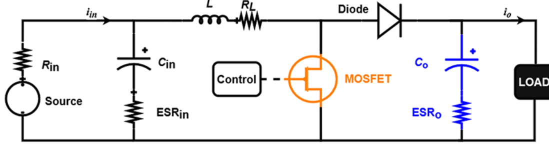

Fig. 2. Boost converter circuit.

Table 1
Converter parameters.

Parameter Variable	Symbol	Value	Units
Input resistance	R_{in}	0.01	Ω
Input capacitance	C_{in}	80	mF
Input capacitor resistance	ESR_{in}	100	mΩ
Inductance	L	146	μH
Inductor internal resistance	R_L	5	mΩ
MOSFET internal resistance	R_{ON}	0.2	Ω
Output Capacitance	C_{o}	5	mF
Output capacitor resistance	ESR_{o}	80	mΩ
Switching frequency	f_s	15	kHz
Input voltage	v_{in}	200	V
Output current	i_{o}	100	A

$$\begin{cases} \dot{x}(t+1) &= A_s x(t) + B_s u(t) + \omega(t), \\ Y(t) &= C_s x(t) + D_s u(t) + \upsilon(t), \end{cases} \tag{1}$$

with:

$$u = \begin{bmatrix} v_{\text{in}} \\ i_{\text{o}} \end{bmatrix}, \quad y = \begin{bmatrix} i_{\text{in}} \\ v_{\text{o}} \end{bmatrix}, \quad x = \begin{bmatrix} v_{C_{\text{in}}} \\ i_L \\ v_{C_{\text{o}}} \end{bmatrix},$$

where, s indicates the switching state of the converter. $x(t) \in \mathbb{R}^{n_x}$ represents the state vectors. $y(t) \in \mathbb{R}^{n_y}$ is the output vector and $u(t) \in \mathbb{R}^{n_u}$ denotes the inputs. $A_s \in \mathbb{R}^{n_x \times n_x}$ represents the state matrix with dim $[A_s(\cdot)] = 3 \times 3$, $B_s \in \mathbb{R}^{n_x \times n_u}$ is the input matrix with dim $[B_s(\cdot)] = 3 \times 2$, $C_s \in \mathbb{R}^{n_y \times n_x}$ is the output matrix with dim $[C_s(\cdot)] = 2 \times 3$ and $D_s \in \mathbb{R}^{n_y \times n_u}$ represents the feed-through matrix of the system with dim $[D_s(\cdot)] = 2 \times 2$; with $\mathbb{R}^n$ is a set of n-dimensional real numbers. $\omega \in \mathbb{R}^{n_x}$ and $\upsilon \in \mathbb{R}^{n_y}$ are the process and measurement noises which are assumed to follow a Gaussian distribution with independent zero mean with covariances Q and R respectively. Additionally, the variable v_{in} is the input source voltage of the circuit, i_{o} is the output load current, i_{in} is the input current and v_{o} is the output voltage. Thus, the states are the input capacitor voltage v_{Cin}, the inductor current i_{L} and v_{Co} the output capacitor voltage.

Therefore, the system splits into two subsystems due to the switching in the converter, and similarly for the buck operation. The ON-state of the Boost operation is represented by subsystem 1 as shown in Fig. 3 and its state-space matrices are derived as follows [18,19]:

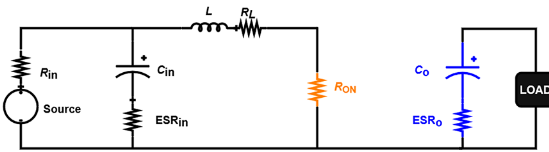

Fig. 3. Boost converter circuit ON-state.

Applying Kirchhoff's Voltage Law (KVL) to subsystem 1, it follows:

$$-v_{\text{o}} + \text{ESR}_{\text{o}} i_{C_{\text{o}}} + v_{C_{\text{o}}} = 0, \tag{2a}$$

$$-v_{\text{in}} + R_{\text{in}} i_{\text{in}} + R_{iC_{\text{in}}} i_{C_{\text{in}}} + v_{C_{\text{in}}} = 0, \tag{2b}$$

$$-v_{\text{in}} + R_{\text{in}} i_{\text{in}} + R_L i_L + v_L + R_{\text{ON}} i_L = 0, \tag{2c}$$

next, by applying Kirchhoff's Current Law (KCL) to subsystem 1:

$$-i_{\text{in}} + i_{C_{\text{in}}} + i_L = 0, \tag{3a}$$

$$i_{C_{\text{o}}} + i_{\text{o}} = 0, \tag{3b}$$

the states equations are then obtained from the above equations:

$$\frac{dv_{C_{\text{in}}}}{dt} = -\frac{1}{C_{\text{in}}(R_{\text{in}} + \text{ESR}_{\text{in}})}[v_{C_{\text{in}}} + R_{\text{in}} i_L - v_{\text{in}}], \tag{4a}$$

$$\frac{di_L}{dt} = \frac{1}{L(R_{\text{in}} + R_{C_{\text{in}}})}[R_{\text{in}} v_{C_{\text{in}}} - (R_{\text{in}} ESR_{\text{in}} + R_L R_{iC_{\text{in}}} + R_{ON} R_{iC_{\text{in}}}) i_L + \text{ESR}_{\text{in}} v_{\text{in}}], \tag{4b}$$

$$\frac{dv_{C_{\text{o}}}}{dt} = -\frac{1}{C_{\text{o}}} i_{\text{o}}, \tag{4c}$$

given the measurement equations as follows:

$$i_{\text{in}} = i_L + C_{\text{in}} \frac{d_{v_{C_{\text{in}}}}}{dt}, \tag{5a}$$

$$v_{\text{o}} = v_{C_{\text{o}}} - \text{ESR}_{\text{o}}\ i_{\text{o}}. \tag{5b}$$

Thus, the state-space matrices of the ON-state Boost converter are represented as follows:

$$A_1 = \begin{bmatrix} \frac{-1}{C_{in} \cdot R_{iC_{in}}} & \frac{-R_{in}}{C_{in} \cdot R_{iC_{in}}} & 0 \\ \frac{R_{in}}{L \cdot R_{iC_{in}}} & \frac{-R_{in} \cdot \text{ESR}_{in} + R_L \cdot R_{iC_{in}} + R_{\text{ON}} \cdot R_{iC_{in}}}{L \cdot R_{iC_{in}}} & 0 \\ 0 & 0 & 0 \end{bmatrix},$$

$$B_1 = \begin{bmatrix} \frac{1}{C_{in} \cdot R_{iC_{in}}} & 0 \\ \frac{R_{C_{in}}}{L \cdot R_{iC_{in}}} & 0 \\ 0 & \frac{-1}{C_{\text{o}}} \end{bmatrix}, \quad C_1 = \begin{bmatrix} \frac{-1}{R_{iC_{in}}} & \frac{\text{ESR}_{in}}{R_{iC_{in}}} & 0 \\ 0 & 0 & 1 \end{bmatrix},$$

$$D_1 = \begin{bmatrix} \frac{1}{R_{iC_{in}}} & 0 \\ 0 & -\text{ESR}_{\text{o}} \end{bmatrix}, \tag{6}$$

Similarly, the OFF-state equations and state-space matrices of subsystem 2 shown in Fig. 4 are obtained as follows [18,19]:

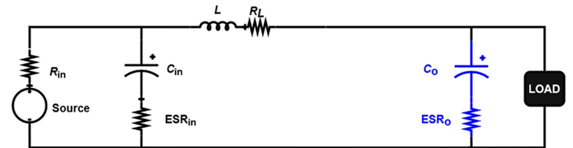

Fig. 4. Boost converter circuit OFF-state.

Applying Kirchhoff's Voltage Law (KVL) to subsystem 2, it yields to:

$$-v_{\text{in}} + R_{\text{in}} i_{\text{in}} + v_L + R_L i_L + v_{C_{\text{o}}} + \text{ESR}_{\text{o}} i_{C_{\text{o}}} = 0, \tag{7}$$

analogously, applying Kirchhoff's Current Law (KCL) to subsystem 2 it follows:

$$-i_L + i_{C_{\text{o}}} + i_{\text{o}} = 0, \tag{8}$$

hence, the state-space matrices of the OFF-state Boost converter are represented as follows:

$$\frac{di_L}{dt} = \frac{R_{\text{in}}}{LR_{iC_{\text{in}}}} v_{C_{\text{in}}} - \frac{R_{\text{in}} ESR_{\text{in}} + R_L R_{iC_{\text{in}}} + ESR_{\text{o}} R_{ic_{\text{in}}}}{LR_{iC_{\text{in}}}} i_L - \frac{v_{C_{\text{o}}}}{L} + \frac{ESR_{\text{in}}}{LR_{ic_{\text{in}}}} v_{\text{in}} + \frac{ESR_{\text{o}}}{L} i_{\text{o}}, \tag{9a}$$

$$\frac{dv_{C_{\text{o}}}}{dt} = \frac{i_L}{C_{\text{o}}} - \frac{i_{\text{o}}}{C_{\text{o}}}, \tag{9b}$$

$$v_o = \mathrm{ESR_o}\ i_L + v_{C_o} - \mathrm{ESR_o}\ i_o. \tag{9c}$$

Thus, the state-space matrices of the OFF-state Boost converter are represented as follows:

$$A_2 = \begin{bmatrix} \frac{-1}{C_{in}\cdot R_{iC_{in}}} & \frac{-R_{in}}{C_{in}\cdot R_{iC_{in}}} & 0 \\ \frac{R_{in}}{L\cdot R_{iC_{in}}} & \frac{-R_{in}\cdot \mathrm{ESR}_{in} + R_L\cdot R_{iC_{in}} + \mathrm{ESR_o}\cdot R_{iC_{in}}}{L\cdot R_{iC_{in}}} & \frac{-1}{L} \\ 0 & \frac{1}{C_o} & 0 \end{bmatrix},$$

$$B_2 = \begin{bmatrix} \frac{1}{C_{in}\cdot R_{iC_{in}}} & 0 \\ \frac{\mathrm{ESR}_{in}}{L\cdot R_{iC_{in}}} & \frac{\mathrm{ESR_o}}{L} \\ 0 & \frac{-1}{C_o} \end{bmatrix}, \quad C_2 = \begin{bmatrix} \frac{-1}{R_i C_{in}} & \frac{\mathrm{ESR}_{in}}{R_{iC_{in}}} & 0 \\ 0 & \mathrm{ESR_o} & 1 \end{bmatrix},$$

$$D_2 = \begin{bmatrix} \frac{1}{R_{iC_{in}}} & 0 \\ 0 & -\mathrm{ESR_o} \end{bmatrix}, \tag{10}$$

where $R_{iCin} = R_{in} + \mathrm{ESR_{in}}$.

This model describes a dynamical system with two operating states which can be expressed as 1) averaged model or 2) alternating model. The first model results the average of the signals in the two operating states with respect to the duty cycle, while the alternating model keeps the ripples of the signals. However, the latter could be beneficial for some applications but previous work shows that the averaged model consumes less computational time and effort and it is more efficient [1].

The following state-space equations represent the averaged model:

$$\begin{aligned} A_{avg} &= A_1\cdot d + A_2\cdot(1-d), \\ B_{avg} &= B_1\cdot d + B_2\cdot(1-d), \\ C_{avg} &= C_1\cdot d + C_2\cdot(1-d), \\ D_{avg} &= D_1\cdot d + D_2\cdot(1-d), \end{aligned} \tag{11}$$

where $d = 0.35$ is the duty cycle that commands the switch.

4. Failure mechanisms of power electronic devices

4.1. Causes of electronics-system failure

Modern power electronic devices have discrete characteristics and are expected to live longer due to the advanced technologies in this field [20]. However, they are exposed to harsh operating conditions which lead to system failure throughout the time. Whereas, the intermittent faults fall outside the scope of this paper, the focus is on the slow deterioration of the most effective power electronic components in the system. Thus, statistical studies have shown that the power switching devices are the most fragile followed by the ECaps [1]. Both of them have been tested by run-to-failure experiments in order to establish the main causes of the occurred faults. Hence, their fault precursors are categorized to facilitate the analytical study. Furthermore, due to the collected results, the experts have categorized the failure mechanisms and types for the power switching devices as in Refs. [9,21]. Similarly, the ECaps have been examined to outline their features [4,5,10]. Henceforth, only the slow parameter variations will be focused on as a type of causes of electronic-systems failure. Thus, the fundamental interest for such failure identification is by pointing out the AGE.

4.2. Accelerated aging experiments

Also known as Accelerated Life Test (ALT), the AGE is a powerful technique to build a data-base of the degradation behavior of the electronic components. Although the power electronic devices run through harsh operating conditions and degrade, they serve the system for a relatively long time. The AGE allow easier investigation of the faults and test the capabilities of the components under test. Furthermore, the reliability assessment is based on the run-until-failure tests with several measurements. These measurements indicate various fault precursors which will be used in the analytical study. Moreover, in-situ measurements are required for the accelerated aging process for both capacitors and power switches [9,16].

The MOSFET module is utilized in the case study of this article. Thus, to analyze its Physics of Failure (PoF), the switching devices should experience electrical and mechanical over-stress. From an engineering point of view, these tests are performed throughout power and thermal cycling to shorten the timescale of the power switching devices. The performed in-situ measurements reports the occurred variations to illustrate their evolution [11–13,22–24].

Moreover, the assessment of the ECaps require special instrumentation. The experiments of the thermal cycling are emulated in a controlled temperature chamber where the temperature is raised over the rated threshold [5]. The age of the ECaps is also accelerated by applying a square voltage higher than its rated with very small frequency [4]. Thus, the thermal over-stress test environment is similar to what has been explained for the MOSFET accelerated aging.

4.3. Failure mechanisms and fault precursors of IGBTs & MOSFETs

The AGE is engaged in the identification of the fault precursors of the tested components. Several experiments have shown that the best indicator of degradation identification in power MOSFETs is the increase in its ON-resistance (R_{ON}) [25] with a margin of 10% to 17% [26]. Another fault precursor for MOSFETs is the increase of the gate threshold voltage [23,27]. Therefore, the fault precursors of IGBTs can be characterized as increase in threshold voltage [28]. The turn-OFF time was also considered as a latch-up indicator in Ref. [29]. In addition, ON-state voltage was also used as a fault precursor for IGBTs in [28,30,31]. More studies that discuss the fault precursors, fault mechanisms and their measurements, are presented in the literature. Consequently, the researchers have categorized the failures of power switching devices into extrinsic (package-related) such as bond-wire fatigue [32,33], solder fatigue [9,16] and Aluminum reconstruction [9] and intrinsic (chip-related) faults such as electrical overstress, electromigration, latch-up and dielectric breakdown [9,21,23,24,33].

4.4. Failure mechanisms and fault precursors of ECaps

Similar to the power switches, the ECaps are one of the major responsible of the electronic-system failures. Therefore, the electrical and thermal over-stress cause major perturbation in the capacitor normal functionality. The electrolyte inside the capacitor unit evaporates which increases the pressure and decreases the oxide area. Physically speaking, the Equivalent Series Resistance (ESR) of the capacitor increases while its capacitance decreases throughout the degradation process [1,5].

4.5. Failure mechanisms methodologies

Each and every failure mechanism is assigned to fault causes and an affected parameter. Analytical studies require the application of empirical models and knowledge of the Physics-of-failure (PoF). Moreover, these parameters can be assigned to the threshold voltage (V_{th}) and collector emitter voltage (V_{CEON}) of the power switches. Hence, electrical and thermal over-stress might increase the leakage current, cause short circuit, open circuit and loss of gate control for power switching devices [9,33].

Moreover, the degradation effects of the ECaps could be detected by observation of the electrolyte, leakage current and/or increase in the internal pressure [1,10].

In many cases, the instrumentation needed to measure and detect these small variations in all applications could be expensive and impossible to apply. Therefore, the RUL identification of these devices could be estimated depending on simulating the failure mechanisms. A few methods exist in the literature that help on estimating the current operating state of the electronic devices without direct measurements in

real applications. Moreover, these analytical studies require real information of the deteriorated devices for all the types of failure supported by the AGE [9,34].

4.6. Empirical failure identification of power electronic devices

Lifetime prediction analysis is based on the empirical models to simplify the reliability assessment. The PoF-based lifetime models could be used to derive the empirical model of thermal failures [9]. In this article, the failure precursor-based lifetime models are adopted. Consequently, due to extensive data acquisition from the AGE, empirical models have been developed for all the possible failure mechanisms.

4.6.1. Empirical lifetime modeling for MOSFETs

Referring to the aforementioned experimental tests, the R_{ON} is the parameter in use for the degradation estimation. Thus, the measurements are interpreted by the numerical analysis methods to fit them in an empirical function [35]. As a result, the ON-resistance variation indicates the degradation variation for the MOSFET. The empirical variation ΔR_{ON} is described by the following equation an its evolution is shown in Fig. 5:

$$\Delta R_{ON} = a_1(e^{b_1 t} - 1), \tag{12}$$

where $a_1 = 3.7.10^{-4}$ and $b_1 = 3.24.10^{-2}$ are the fitted parameters of the ON-resistance degradation extracted from the AGE measurements.

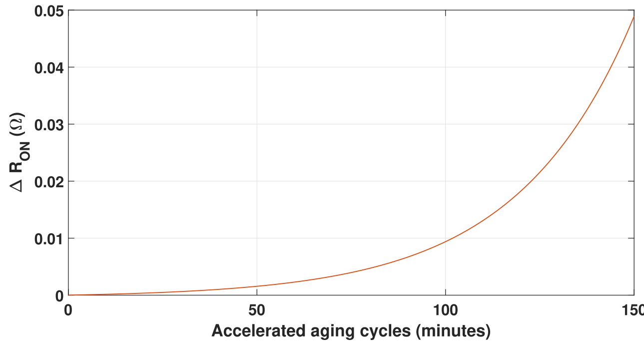

Fig. 5. MOSFET ON-resistance variation due to degradation using empirical model.

In the literature, the researchers tend also to model the fault precursors based on failure mechanisms and PoF as in Ref. [9].

4.6.2. Empirical lifetime modeling for ECaps

The lumped model of the ECaps is expressed by a capacitance and ESR. Hence, for model-based applications, the empirical modeling is interpreted using numerical curve-fitting methods for illustration. Here follows the equations of the capacitance and the ESR of the ECaps [5,36].

$$C = \frac{2\ \varepsilon_R\ \varepsilon_o\ A_o}{t_o}, \tag{13a}$$

$$\mathrm{ESR} = \frac{\rho_E\ t_o\ P_E}{2\ L\ W}, \tag{13b}$$

where ε_R is the relative dielectric constant, ε_o is the permittivity of free space, A_o is the oxide area, t_o is the oxide thickness, ρ_E is the electrolyte resistivity, L and W are the physical parameters of the anode area, P_E is the correlation factor related to electrolyte space porosity and average liquid path-away [5]. Fig. 6 shows the equivalent circuit of lumped ECaps.

The empirical models of capacitance loss and ESR increase according to [17] are given by the following equations:

Fig. 6. Lumped model of electrolytic capacitor.

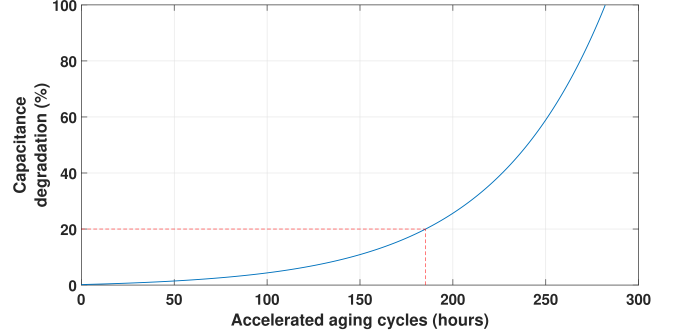

(a) Evolution of capacitance degradation using empirical model.

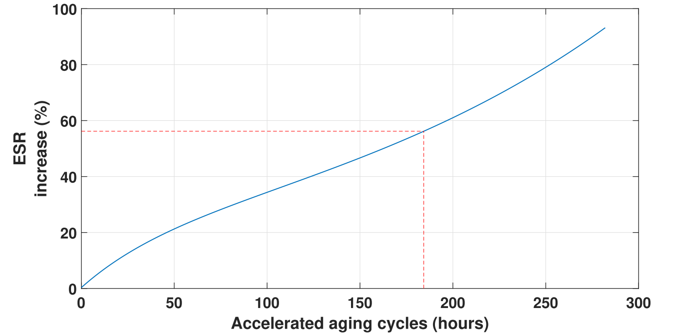

(b) Evolution of ESR using empirical model.

Fig. 7. Evolution of the lumped model of ECaps.

$$C_{\deg}(t) = e^{a_2 t} + b_2, \tag{14a}$$

$$\mathrm{ESR}_{\mathrm{inc}}(t) = a_3 e^{b_3 t} + c_3 e^{d_3 t}, \tag{14b}$$

similarly to the aforementioned parameters of the ON-resistance, $a_2 = 0.0163$, $b_2 = -0.8398$, $a_3 = 21.91$, $b_3 = 0.005117$, $c_3 = -22.2$ and $d_3 = -0.02211$ are the fitted parameters of the capacitor degradation extracted from the AGE measurements. Fig. 7a and b show the evolution of the empirical models considering the capacitance degradation and ESR increase percentages.

It should be noted that the maximum threshold of the capacitance degradation is 20% of the initial capacitance value, based on the aforementioned experiments. Consequently, the ESR increases by 57% for a 20% of capacitance degradation.

5. Proposed PHM approach

5.1. Degradation estimation using adaptive joint extended Kalman filter

The aforementioned intrinsic and extrinsic failures have been defined to employ the simulation of the empirical models in order to estimate the degradation of the components as well as the overall system. Moreover, the reliability assessment should be trustworthy based on efficient estimation method. Therefore, due to the characteristics of each electronic device, the deterioration speed of the components oblige to split the system into different manifolds. Hence, the fast manifold is directly related the states of the system on which linear filtering techniques could be applied. Whereas, the slow manifold emulates the degradation of the internal parameters which are characterized by smooth variations. Consequently, the slow manifolds impose an assumption of $\delta_{k+1} = \delta_k + \mathrm{r}_k$, where δ denotes the variations of the

parameters and r_k is a small white noise.

To reflect the degradation of the internal components on the whole system, the variations should be measured. Hence, dealing with a black box system, the internal components are not accessible for sensor measurements. Therefore, the proposed estimation is employed for auto-adaptive parameters update. To do so, the model-based implementation allows to augment the states with the parameters. In Ref. [1], two estimation techniques were employed where the AJEKF technique shows better results than the ADKF. Thus, it will be described and utilized for the case study.

It should also be noted that infecting the model by the empirical degradation models is only used for simulation validation purposes in the absence of real system degradation.

Consider the parameter-variant nonlinear discrete model of the following form:

$$\begin{cases} x_{k+1} &= A_i(\delta_k)x_k + B_i(\delta_k)u_k + \omega_k, \\ y_k &= C_i(\delta_k)x_k + D_i(\delta_k)u_k + \upsilon_k, \end{cases} \tag{15}$$

Henceforth, this model will be denoted as the augmented system due to the augmented parameter δ. where, $i = 1$ indicates the selection of subsystem 1, $i = 2$ indicates the selection of subsystem 2, and $i = avg$ is the average model used for parameter estimation.

After augmenting the system with the parameter δ, the states vector becomes:

$$x_k^{aug} = \begin{bmatrix} x^{old} \\ \delta \end{bmatrix} \tag{16}$$

For simplification purposes, $k|k-1$ is denoted as k^- and $k|k+1$ is denoted as k^+, $A_k{}^{aug}$ as A_k with the rest of the state-space matrices. Hence, the dimensions of the state-space matrices change as follows:

dim $[A(\cdot)] = 4 \times 4$, dim $[B(\cdot)] = 4 \times 2$, dim $[C(\cdot)] = 2 \times 4$ and dim $[D(\cdot)] = 4 \times 2$.

The filtering of the non-linear augmented system is solved by applying the conventional Kalman filtering method with a few modifications (AJEKF). Hence, the linearization process involves the Jacobian of f and g denoting the matrices A and C. The Jacobian matrices are calculated for each subsystem first and then the average model is computed. The model is discretized and a conventional KF is applied for the average subsystem as shown in the following equations:

The state estimate time update:

$$x_k = A_{k^-}x_{k^-} + B_{k^-}u_{k^-} + \omega_{k^-}, \tag{17}$$

The prediction error covariance:

$$P_k = \frac{\partial f}{\partial x}\bigg|_{\hat{x}_{k^-}} P_{k^-} \frac{\partial f^T}{\partial x}\bigg|_{\hat{x}_{k^-}} + Q, \tag{18}$$

Kalman gain:

$$K_k = P_{k^-}\left(\frac{\partial g_{x_{k^-}}}{\partial x}\right)^T \times \left[\left(\frac{\partial g_{x_{k^-}}}{\partial x}\right)P_{k^-} \times \left(\frac{\partial g_{x_{k^-}}}{\partial x}\right) + R\right]^{-1} \tag{19}$$

The output equation:

$$y_k = C_{k^-}x_{k^-} + D_{k^-}u_{k^-} + \upsilon_{k^-}, \tag{20}$$

The filter equation:

$$x_k = x_{k^-} + K_k(Y_k - y_k), \tag{21}$$

The filter error covariance:

$$P_{k^+} = \left(I - K_k\frac{\partial g_{x_k}}{\partial x}\right)P_k, \tag{22}$$

5.2. PHM architecture

The early warnings are considered as the fundamental features of the prognostics. Although the decision-making process has never been an easy mission, there are historical and current signs that help furnishing the prediction links and provide a complete life-cycle update on a component-level and henceforth a system-level [6].

Algorithms alternate among many engineering disciplines for the reason of optimizing the reliability by involving the fault detection, identification, isolation and lately the fault prognostics mostly benefiting the maintenance management.

Here follows the proposed PHM architecture for online RUL forecasting as shown in Fig. 8:

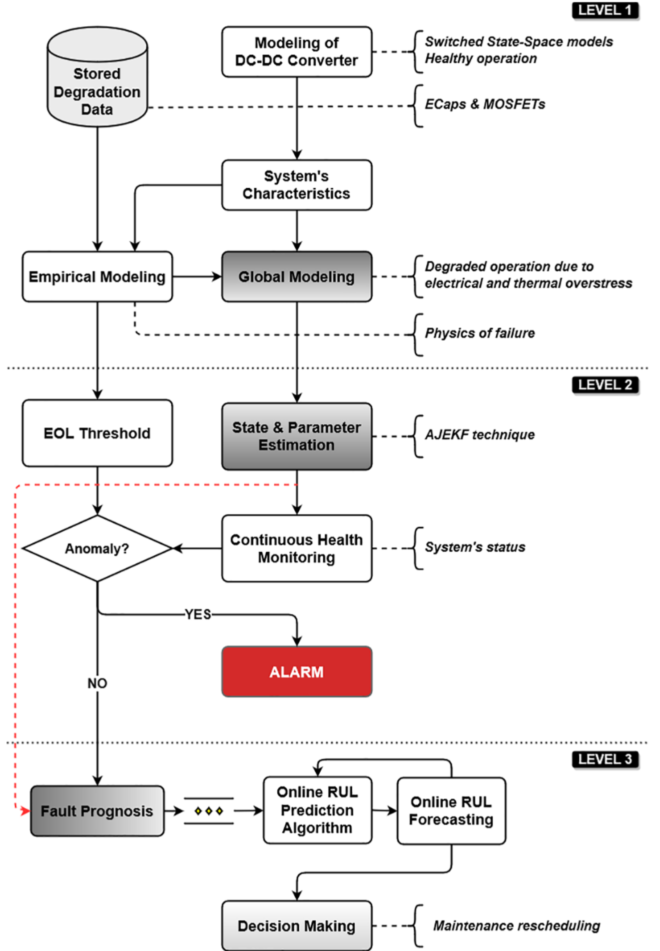

Fig. 8. Proposed PHM architecture.

5.2.1. Level 1: system modeling and features extraction

• The modeling of the plant comes in the healthy operating mode as a first step of the analytical study. Thus, it is crucial to specify the sensors and the measurement devices precision and noise power for further applications. As shown before, the DC-DC converter was split into two state-space models describing its functionality with respect to the process and measurement noises.

• The system characteristics are important to extract the environmental working conditions, the limitations of the parameters in order to establish a study about their physics of failure.

• The AGE help building a database used for statistical analysis of the behavior of the power electronic components. Thus, the degradation analysis is numerically calculated for the next step. The degradation data are available online from the data repository of the prognostics center of Nasa.

• The previous step leads to generalize degradation equations for each and every tested electronic components. Hence, empirical models adapt the healthy operation mode to create the degraded state-space

models of the whole power electronic system.

• Lately in level 1 of the prognosis study, a global model has to be generated either in model-based or data-driven techniques for the simulation study of the PHM.

5.2.2. Level 2: parameter estimation and health monitoring

• The AJEKF technique is responsible of estimating the states of the global model for the $k + 1$ state. In parallel, the slow-variation are also estimated using advanced filtering techniques since their degradation could not be directly detected.

• Prior knowledge of the system could help to define an end-of-life threshold based on the experimental results.

• The system is continuously monitored to detect any sudden fault, allocate it and then isolate it. This process is traditionally known as fault diagnosis and it is based on the estimation done in the previous step. In case of a fault, the system will take decision by a human interface or it could be self-cleared depending on its intensity. However, for the non-faulty condition, the prognosis algorithm will take place in order to estimate the RUL of the system.

5.2.3. Level 3: RUL forecasting

Independently of the degradation knowledge, the RUL forecasting algorithm considers the estimated parameters only. At each time step, the fault prognosis algorithm fits the measured parameter with a polynomial equation which updates its variables at each iteration. A linear EoL-RUL equation is optimistically assumed in the prognosis profile. Moreover, the algorithm runs in online mode and it converges at each iteration. It is also assumed that the component break-through threshold is the stopping criterion, the EoL of the system. Therefore, the expected results are the RUL in function of operating time. The simulation results in Section 6, numerically explains the robustness of this proposed technique. Additionally, the EoL of the whole system is assumed at the time where one critical device in the system fails. Thus, the system-level RUL is the RUL of the first-to-fail component. Here follows the algorithm to compute the RUL:

Algorithm 1. RUL forecasting algorithm.

Output: forecasting of the prognosis horizon.

Prerequisites :

- At $k = 1$, assume that the EoL of the system is the same as the expected operation time by the user.
- The previously assumed time is considered as the threshold of the parameter degradation. Consequently, the system is then considered as 100% degraded from its initial state.

1: **for** $k = 1$ to $\mathbb{N}$ **do**
2: The polynomial equation will consider the estimated state with the current deviation of the initial state
3: Computation of the variables of the polynomial equations
4: Update and calculation of the EoL
5: Deduction of the value of RUL: "EoL$-k\times$simulation time"
6: Update the variables and repeat until reaching the threshold
7: **end for**
8: **return** the RUL at each measurement.

6. Simulation results

Algorithm 1 of RUL forecasting is mainly implemented for the final level of the proposed PHM algorithm and it is based on the parameter estimation. Therefore, it is essential to run simulation tests in order to assess the validity of the proposed prognostics algorithm. Both of the degradation cases were tested on the DC-DC converter in Boost operation mode. The AJEKF technique was applied for states and parameter estimation. The ESR of the output capacitor and the ON-resistance of the MOSFET are considered as the degraded parameters that infect the model. It should be noted that the empirical models of the degraded parameters are only used in simulation to infect the model with slow degradation data which are already measured by real AGE. Two different colors are used to visualize the simulation results in order to differentiate between ECaps and MOSFET degradation. The states are initialized with random values such as 50, 100 and 200 for input capacitance voltage, inductor current and output capacitor voltage respectively while their ideal values in normal operation mode are 200 V, 150 A and 300 V. Thus, the input voltage is set to 200 V and the output current is 100 A. At $k = 1$, the state-space matrices are computed with the initial value of the degraded parameter $\delta_0 = ESR_0 = 80$ mΩ or $\delta_0 = R_{ON} = 0.2$ Ω.

6.1. DC-DC converter parameters estimation during capacitor degradation

As known, the output capacitor has a direct effect on the output voltage value as well as the voltage ripples. However, the proposed estimation technique ignores the voltage ripples by averaging the equations of the two subsystems.

Fig. 9a shows the degradation occurring at the output capacitor voltage during the capacitor degradation along with Fig. 9b that represents the output voltage. Thus, it can be seen that the output components voltages are directly affected by the degradation and both represent a voltage drop of around 4 V. The small box shows a zoomed view of the degraded as well as the estimated states.

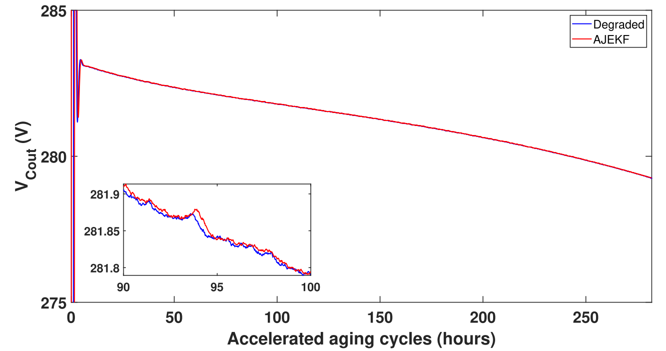

(a) Output capacitor voltage during capacitor degradation.

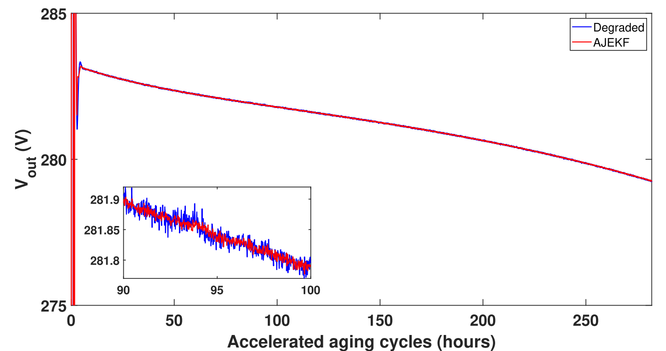

(b) Output voltage during capacitor degradation.

Fig. 9. Output components voltages during capacitor degradation.

The input capacitor voltage is independent of the degradation of the output capacitor as shown in Fig. 10. However, Fig. 11 shows the 2 A drop of the inductor current from its initial real and estimated value. Thus, this can be explained by the second element of the input vector u, the output current. Since the load is constant, the output current drops with the output voltage. Consequently, most of the components are affected due to the inter-connections of the system.

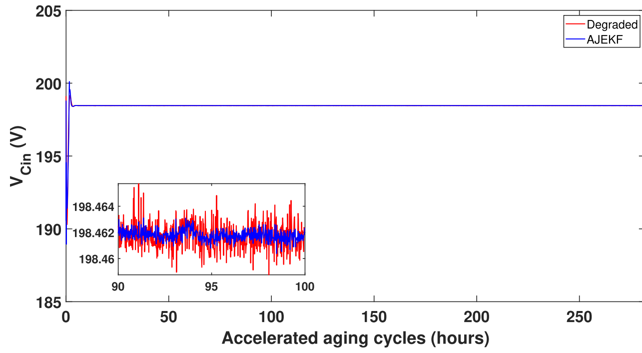

Fig. 10. Input capacitor voltage during capacitor degradation.

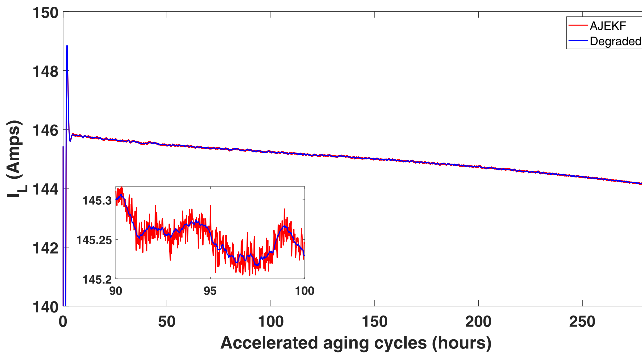

Fig. 11. Inductor current during capacitor degradation.

Moreover, as detailed in the empirical models, the ESR increases with the capacitance degradation. Thus, the AJEKF proves its ability to estimate the small-varied parameter of the system as shown in Fig. 12. Only the values of the parameter estimation will be used in the level 3 of the PHM algorithm for RUL forecasting.

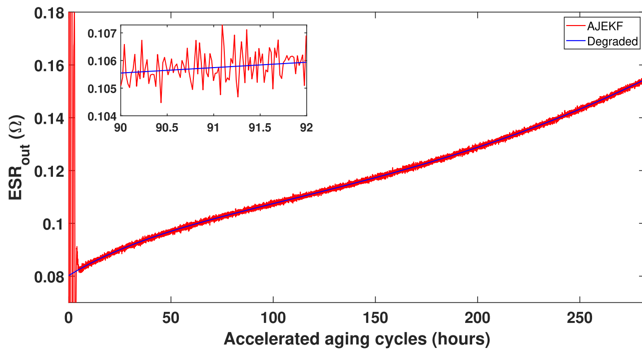

Fig. 12. ESR_o estimation during capacitor degradation.

6.2. DC-DC converter parameters estimation during MOSFET degradation

The empirical models were simulated with the AJEKF estimation technique and the results are presented below:

Similar to the capacitor degradation case, only the output voltage and output capacitor voltage are affected by the capacitor degradation as shown in Fig. 13a and b.

Despite the system inter-connections, Fig. 14 shows intact input capacitor voltage during the degradation process. Thus, similar to the case of the capacitor degradation, the inductor current is also affected by the degradation of MOSFET where Fig. 15 shows 2 A current drop for the same reasons explained in the capacitor degradation case.

As the MOSFET is characterized by its ON-resistance, the latter is used for the estimation algorithm in the case of MOSFET degradation. Hence, Fig. 16 demonstrates the increase in resistance by 0.03 Ω and the parameter estimation as well.

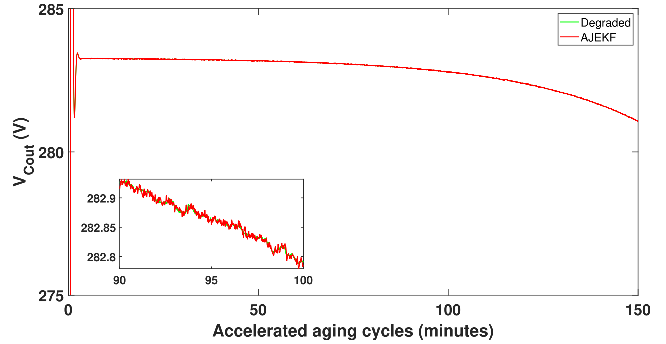

(a) Output capacitance voltage during MOSFET degradation.

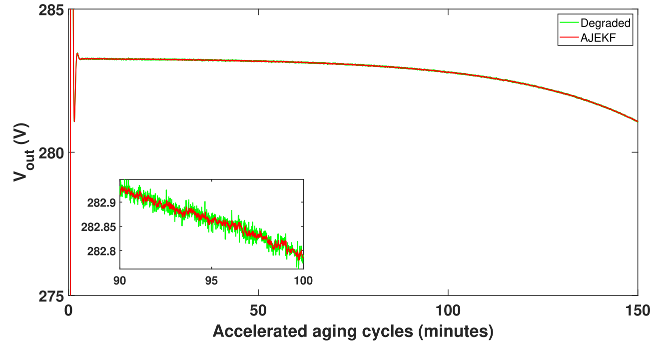

(b) Output voltage during MOSFET degradation.

Fig. 13. Output components voltages during MOSFET degradation.

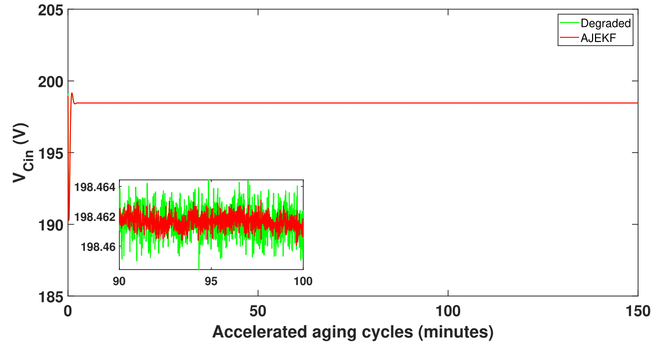

Fig. 14. Input capacitance voltage during MOSFET degradation.

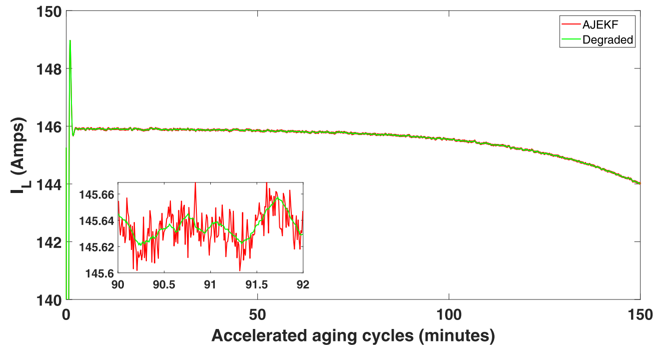

Fig. 15. Inductor current during MOSFET degradation.

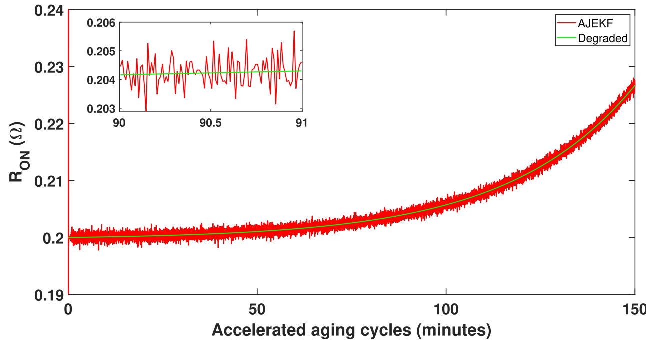

Fig. 16. R_{ON} estimation during MOSFET degradation.

6.3. Online RUL forecasting

The essential results of the PHM algorithm are demonstrated in Fig. 17. The RUL prediction algorithm runs in parallel with the parameter estimation process. At each time-step, the proposed polynomial fit of the earlier estimation computes the current RUL based on the aforementioned assumptions and conditions. As clearly shows the blue line, the prediction converges to the empirical ideal EoL in red which is only used in simulation as a base to compare the proposed method with the ideal EoL-RUL function.

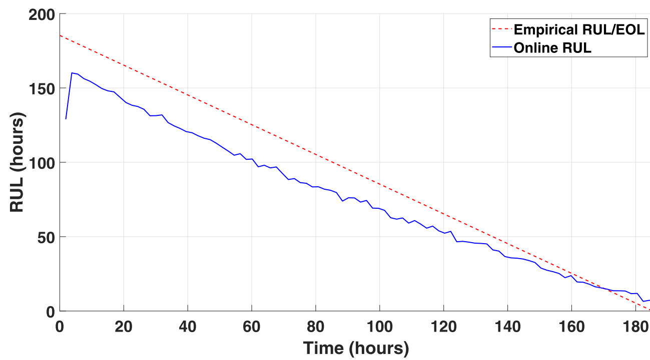

Fig. 17. Online RUL forecasting during capacitor degradation. (For interpretation of the references to color in this figure, the reader is referred to the web version of this article.)

Furthermore, Fig. 18 shows the prediction error at each measurement time between the empirical RUL-EoL used only for simulation purposes and the predicted RUL. Moreover, researchers in [4,10,14,15] used the relative accuracy as an indicator of prediction accuracy. Thus, the latter is also computed and showed in Fig. 19.

$$\mathrm{RA}_{\%} = 100 - \frac{|\mathrm{RUL}_k^{pred} - \mathrm{RUL}_k|}{\mathrm{RUL}_k} \times 100, \tag{23}$$

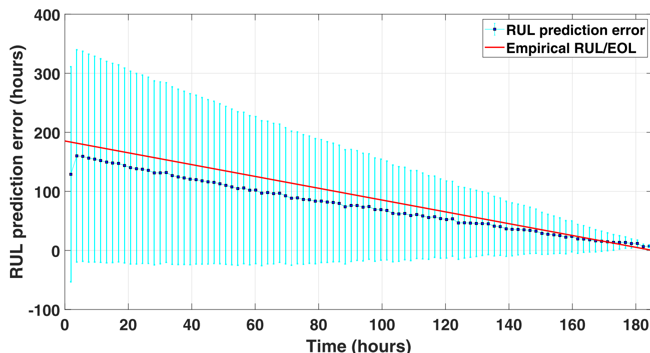

Fig. 18. Error of online RUL prediction.

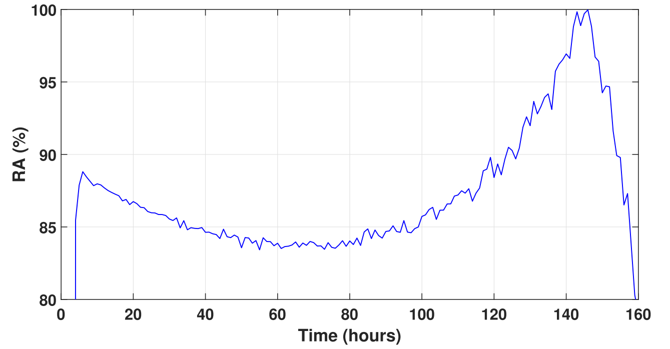

Fig. 19. The relative accuracy of the RUL prediction with respect to the empirical model.

the higher the RA percentage is, the more the prediction with respect to RUL is accurate.

7. Conclusion

This paper highlights the proposed methodology of RUL prediction of an electronics-rich system from a component to system-level without prior knowledge of the degradation behaviors of the components. It is crucial to understand the failure mechanisms of the power electronic components to deal with system-level prognostics especially in simulation to be able to infect the model with empirical degradation models. The proposed model-based PHM methodology splits the architecture into three stages: modeling, estimation and prediction. Thus, Extended Kalman filtering is applied in order to estimate the states and the degraded parameters by augmenting the states vector. Straightforward to the problem, the RUL prediction of the whole system is based on the first-to-fail critical device in the system such as MOSFETs/IGBTs and ECaps. Finally, the simulation shows high accuracy estimation and prediction enhanced by the proposed PHM technique to deal with such systems. Current and future work will focus on other techniques such as interval predictors and zonotopes which will be validated on a real test bench with the previous research.

Credit author Statement.

Ahmad Al-Mohamad: term, Conceptualization, Methodology, Software, Validation, Formal analysis, Investigation, Resources, Data curation, Writing - original draft, Writing - review & editing, Visualization.

Ghaleb Hoblos: Conceptualization, Validation, Resources, Writing - review & editing, Supervision, Project administration, Funding acquisition.

Vicenç Puig: Conceptualization, Validation, Resources, Writing - review & editing, Supervision, Project administration, Funding acquisition.

Declaration of competing interests

The authors declare that they have no known competing financial interests or personal relationships that could have appeared to influence the work reported in this paper.

CRediT authorship contribution statement

Ahmad Al-Mohamad: Conceptualization, Methodology, Software, Validation, Formal analysis, Investigation, Resources, Data curation, Writing - original draft, Writing - review & editing, Visualization.**Ghaleb Hoblos:**Conceptualization, Validation, Resources, Writing - review & editing, Supervision, Project administration, Funding acquisition.**Vicenç Puig:**Conceptualization, Validation, Resources, Writing - review & editing, Supervision, Project administration,

Funding acquisition.

Acknowledgement

This work is co-funded by European Union and Normandy Region. Europe is involved in Normandy through the European Funds for Regional Development.

References

[1] A. Al-Mohamad, G. Hoblos, V. Puig, A model-based prognostics approach for RUL forecasting of a degraded DC-DC converter, 2019 4th Conference on Control and Fault Tolerant Systems (SysTol), 2019, pp. 312–318 , https://doi.org/10.1109/SYSTOL.2019.8864778.

[2] K. Tidriri, S. Verron, T. Tiplica, N. Chatti, A decision fusion based methodology for fault prognostic and health management of complex systems, Appl. Soft Comput. 105622 (2019) 1568–4946, https://doi.org/10.1016/j.asoc.2019.105622 ISSN.

[3] M. Pecht, A Prognostics and Health Management for Information and Electronics-Rich Systems, (2011), pp. 19–30, https://doi.org/10.1007/978-0-85729-493-7.

[4] C.S. Kulkarni, J.R. Celaya, G. Biswas, K. Goebel, Prognostics of power electronics, methods and validation experiments, 2012 IEEE Autotestcon Proceedings, 2012, pp. 194–199, , https://doi.org/10.1109/AUTEST.2012.6334578 ISSN 1558-4550.

[5] C. Kulkarni, J. Celaya, G. Biswas, K. Goebel, Prognostic modeling and experimental techniques for electrolytic capacitor health monitoring, Structural Health Monitoring 2011: Condition-Based Maintenance and Intelligent Structures — Proceedings of the 8th International Workshop on Structural Health Monitoring, National Aeronautics and Space Administration MOFFETT Field CA AMES Research Center, 2011, pp. 1225–1232.

[6] H.M. Elattar, H.K. Elminir, A.M. Riad, Prognostics: a literature review, Complex Intell. Syst. 2 (2) (2016) 125–154 ISSN 2199-4536 https://doi.org/10.1007/s40747-016-0019-3.

[7] B. Saha, J.R. Celaya, P.F. Wysocki, K.F. Goebel, Towards prognostics for electronics components, 2009 IEEE Aerospace Conference, 2009, pp. 1–7.

[8] M. Pecht, Prognostics and health monitoring of electronics, 2006 International Conference on Electronic Materials and Packaging, 2006, pp. 1–10.

[9] A. Hanif, Y. Yu, D. DeVoto, F. Khan, A comprehensive review toward the state-of-the-art in failure and lifetime predictions of power electronic devices, IEEE Transactions on Power Electronics vol. 34 (5) (2019) 4729–4746.

[10] J. Celaya, C. Kulkarni, G. Biswas, S. Saha, K. Goebel, A model-based prognostics methodology for electrolytic capacitors based on electrical overstress accelerated aging, Annual Conference of the Prognostics and Health Management Society 2011, PHM, Montreal QC, Canada, 2011, pp. 31–39.

[11] Z. Li, Z. Zheng, R. Outbib, A prognostic methodology for power MOSFETs under thermal stress using echo state network and particle filter, Microelectron. Reliab. 88–90 (2018) 350–354, https://doi.org/10.1016/j.microrel.2018.07.137 (29th European Symposium on Reliability of Electron Devices, Failure Physics and Analysis (ESREF 2018).

[12] J.R. Celaya, A. Saxena, S. Saha, V. Vashchenko, K. Goebel, Prognostics of power MOSFET, 2011 IEEE 23rd International Symposium on Power Semiconductor Devices and ICs, 2011, pp. 160–163 , https://doi.org/10.1109/ISPSD.2011.5890815.

[13] J.R. Celaya, A. Saxena, S. Saha, K.F. Goebel, Prognostics of power MOSFETs under thermal stress accelerated aging using data-driven and model-based methodologies, Annual Conference of the Prognostics and Health Management Society 2011, 2011, pp. 443–452.

[14] S. Benmoussa, M.A. Djeziri, Remaining useful life estimation without needing for prior knowledge of the degradation features, IET Sci. Meas. Technol. 11 (8) (2017) 1071–1078, https://doi.org/10.1049/iet-smt.2017.0005.

[15] M.A. Djeziri, S. Benmoussa, R. Sanchez, Hybrid method for remaining useful life prediction in wind turbine systems, Renew. Energy 116 (2018) 173–187, https://doi.org/10.1016/j.renene.2017.05.020 https://doi.org/10.1016/j.renene.2017.05.020.

[16] A. Alyakhni, A. Al-Mohamad, G. Hoblos, Joint estimation of MOSFET degradation in a DC-DC converter using extended Kalman filter, 2019 4th Conference on Control and Fault Tolerant Systems (SysTol), 2019, pp. 319–324 , https://doi.org/10.1109/SYSTOL.2019.8864731.

[17] J.K. Man, S. Perinpanayagam, I. Jennions, Aging detection capability for switch-mode power converters, IEEE Trans. Ind. Electron. 63 (5) (2016) 3216–3227, https://doi.org/10.1109/TIE.2016.2535104.

[18] H. Al-Sheikh, O. Bennouna, G. Hoblos, N. Moubayed, Modeling, design and fault analysis of bidirectional DC-DC converter for hybrid electric vehicles, 2014 IEEE 23rd International Symposium on Industrial Electronics (ISIE), 2163-51452014, pp. 1689–1695 , https://doi.org/10.1109/ISIE.2014.6864869.

[19] D.W. Hart, Power Electronics, McGraw-Hill, 2010.

[20] H. Qingchuan, C. Wenhua, P. Jun, Q. Ping, A prognostic method for predicting failure of dc/dc converter, Microelectron. Reliab. 74 (2017) 27–33 ISSN 00262714 https://doi.org/10.1016/j.microrel.2017.05.014.

[21] J.M. Anderson, R.W. Cox, P. O'Connor, Online algorithm for early stage fault detection in IGBT switches, 2013 9th IEEE International Symposium on Diagnostics for Electric Machines, Power Electronics and Drives (SDEMPED), 2013, pp. 1–8 , https://doi.org/10.1109/DEMPED.2013.6645689.

[22] J.R. Celaya, A. Saxena, P. Wysocki, S. Saha, K. Goebel, Towards prognostics of power MOSFETs: accelerated aging and precursors of failure, Annual Conference of the Prognostics and Health Management Society 2010, 2010 Portland, OR.

[23] S. Saha, J.R. Celaya, V. Vashchenko, S. Mahiuddin, K.F. Goebel, Accelerated Aging with Electrical Overstress and Prognostics for Power MOSFETs, 2011 IEEE, 2011, pp. 1–6, https://doi.org/10.1109/EnergyTech.2011.5948532 EnergyTech.

[24] J.R. Celaya, P. Wysocki, V. Vashchenko, S. Saha, K. Goebel, Accelerated aging system for prognostics of power semiconductor device, 2010 IEEE AUTOTESTCON, 2010, pp. 1–6, , https://doi.org/10.1109/AUTEST.2010.5613564.

[25] L. Dupont, S. Lefebvre, M. Bouaroudj, Z. Khatir, J. Faugieres, F. Emorine, Ageing test results of low voltage MOSFET modules for electrical vehicles, 2007 European Conference on Power Electronics and Applications, 2007, pp. 1–10 , https://doi.org/10.1109/EPE.2007.4417433.

[26] S. Dusmez, B. Akin, An accelerated thermal aging platform to monitor fault precursor on-state resistance, 2015 IEEE International Electric Machines Drives Conference (IEMDC), 2015, pp. 1352–1358 , https://doi.org/10.1109/IEMDC.2015.7409238.

[27] S. Dusmez, S.H. Ali, M. Heydarzadeh, A.S. Kamath, H. Duran, B. Akin, Aging precursor identification and lifetime estimation for thermally aged discrete package silicon power switches, IEEE Trans. Ind. Appl. 53 (1) (2017) 251–260.

[28] N. Patil, D. Das, M. Pecht, A prognostic approach for non-punch through and field stop IGBTs, Microelectron. Reliab. 52 (3) (2012) 482–488 ISSN 0026-2714 https://doi.org/10.1016/j.microrel.2011.10.017 (special section on International Seminar on Power Semiconductors 2010).

[29] D.W. Brown, M. Abbas, A. Ginart, I.N. Ali, P.W. Kalgren, G.J. Vachtsevanos, Turn-off time as an early indicator of insulated gate bipolar transistor latch-up, IEEE Trans. Power Electron. 27 (2) (2012) 479–489 ISSN 1941-0107 https://doi.org/10.1109/TPEL.2011.2159848.

[30] Y. Xiong, X. Cheng, Z.J. Shen, C. Mi, H. Wu, V.K. Garg, Prognostic and warning system for power-electronic modules in electric, hybrid electric, and fuel-cell vehicles, IEEE Trans. Ind. Electron. 55 (6) (2008) 2268–2276 ISSN 1557-9948 https://doi.org/10.1109/TIE.2008.918399.

[31] V. Smet, F. Forest, J. Huselstein, A. Rashed, F. Richardeau, Evaluation of V_{ce} monitoring as a real-time method to estimate aging of bond wire-IGBT modules stressed by power cycling, IEEE Trans. Ind. Electron. 60 (7) (2013) 2760–2770 ISSN 1557-9948 https://doi.org/10.1109/TIE.2012.2196894.

[32] M. Ciappa, Selected failure mechanisms of modern power modules, Microelectron. Reliab. 42 (4) (2002) 653–667 ISSN 0026-2714 https://doi.org/10.1016/S0026-2714(02)00042-2.

[33] N. Valentine, D. Das, P.M. Pecht, Failure mechanisms of insulated gate bipolar transistors (IGBTs), 2015 NREL Photovoltaic Reliability Workshop, 2015.

[34] W. Denson, The history of reliability prediction, IEEE Trans. Reliab. 47 (3) (1998) SP321–SP328 ISSN 1558-1721 https://doi.org/10.1109/24.740547.

[35] J.R. Celaya, A. Saxena, C.S. Kulkarni, S. Saha, K. Goebel, Prognostics approach for power MOSFET under thermal-stress aging, 2012 Proceedings Annual Reliability and Maintainability Symposium, 2012, pp. 1–6 , https://doi.org/10.1109/RAMS.2012.6175487.

[36] C.S. Kulkarni, G. Biswas, J.R. Celaya, K. Goebel, Physics based electrolytic capacitor degradation models for prognostic studies under thermal overstress, European Conference of the Prognostics and Health Management Society, 4 2012, pp. 1–9 (1). ISSN 21532648, URL, http://www.phmsociety.org/node/936.